Available online at www.sciencedirect.com
SCIENCE DIRECT®
Acta Materialia 53 (2005) 2901–2907
Acta MATERIALIA
www.actamat-journals.com

Transition between low and high angle grain boundaries

Myrjam Winning [a,*], Anthony D. Rollett [b]

[a] Institut für Metallkunde und Metallphysik, RWTH Aachen, Kopernikusstr. 14, 52056 Aachen, Germany
[b] Carnegie Mellon University, Pittsburgh, PA 15213, USA

Received 27 September 2004; received in revised form 2 March 2005; accepted 4 March 2005
Available online 18 April 2005

Abstract

The migration of planar, symmetric tilt grain boundaries with different tilt axes was investigated. The driving force for the grain boundary migration was due to an external mechanical stress field. Low as well as high angle grain boundaries can move under this driving force and the activation parameters for the stress induced grain boundary motion are different for low and high angle grain boundaries. The experiments showed a sharp transition from low angle grain boundary to high angle grain boundary behavior. The transition is marked by a clear change in the activation enthalpy for the grain boundary motion without any extended range. We present an overview of the existing experimental results and theoretical considerations of the structure of grain boundaries at the transition. The observation that the transition depends on the rotation axis of the grain boundary and on the grain boundary plane is particularly important, because this will influence the Brandon criterion which is often used in experiments and simulations of grain growth and recrystallization processes.

Keywords: Transition angle; Low angle grain boundaries; High angle grain boundaries; In situ observations; X-ray diffraction

1. Introduction

According to conventional grain boundary theory, the transition from low angle to high angle grain boundaries occurs at a transition angle in the range of 10–20°, but is not known exactly. On the one hand, experiments determining grain boundary energies [1–3] suggest a transition angle near 15°. On the other hand, one can still discern single dislocations in grain boundaries with misorientation angles near 20° by high resolution imaging [4]. There exist neither experimental data nor theoretical concepts to determine the transition angle exactly.

Recently, it was shown that planar tilt boundaries with different tilt axes (⟨1 1 2⟩, ⟨1 1 1⟩ and ⟨1 0 0⟩) can be moved by an external mechanical shear stress, irrespective whether the boundary is a low angle or a high angle grain boundary [5–7]. In these experiments, it was also found that there exists a sharp transition from low angle to high angle boundaries which could be identified by a conspicuous step in the activation enthalpy at an angle of 13.6° for both ⟨1 1 2⟩- and ⟨1 1 1⟩ tilt axes, but at an angle of 8.6° for the ⟨1 0 0⟩-tilt axis. From these experiments, it seems that the transition angle depends on the orientation of the respective tilt axis.

In this study, experiments are presented where the grain boundaries have a ⟨1 0 0⟩-tilt axis, but in contrary to the experiments in [7], the direction of the grain boundary plane normal was different. The results of these experiments show that the transition angle is approximately 14.4° which is comparable to the results in [5,6] and different to the transition angle which was found in [7].

* Corresponding author. Tel.: +49 241 802 6899; fax: +49 241 802 2301.
E-mail address: winning@imm.rwth-aachen.de (M. Winning).

1359-6454/$30.00
doi:10.1016/j.actamat.2005.03.005

Therefore, the aim of this study is to provide a quantitative explanation of the transition angle from low angle to high angle behavior and to rationalize the existence of distinct different transition angles in terms of a critical dislocation density at the transition angle for the different investigated tilt axes.

2. Experimental procedure

2.1. Measurement of grain boundary migration and application of stress

To measure the grain boundary motion, a special X-ray diffraction tracking device was used [8] which allows the grain boundary position to be located continuously without interruption of the migration process. The specimen holder (see Fig. 1 [7]) was designed such as to exert a shear stress parallel to the grain boundary normal. In order to apply the shear stress, a spring with a well-defined spring constant is compressed. This compression leads to a definite displacement of the upper grip in Fig. 1. The lower grip is fixed so that the displacement of the upper grip causes shear stresses at the sample and at the grain boundary which are parallel to the grain boundary plane normal. The methods used to activate the migration of planar grain boundaries and the in situ measurement of the stress-induced grain boundary motion are described in detail in [5,7]. It should be noted that the experiments showed that low angle as well as high angle grain boundaries move under the applied shear stress and that a steady-state motion of the grain boundaries could be measured. Therefore, we could determine the grain boundary velocity from the displacement–time diagrams and it was found that grain boundary velocity and external shear stress are proportional.

2.2. Investigated grain boundaries

High purity aluminium bicrystals were used for the experiments with a total impurity content of 7.7 and 1 ppm, respectively. The bicrystals were grown from the melt by using a modified Bridgman technique. The investigated grain boundaries were planar, symmetric tilt grain boundaries with misorientation angles between 3–34° and different tilt axes (⟨1 1 2⟩-, ⟨1 1 1⟩- and ⟨1 0 0⟩ tilt axes). The different orientations of the analyzed bicrystals are shown in Fig. 2. In the following, we assume that each symmetric tilt grain boundary contains only edge dislocations [1], which are the geometrically necessary dislocations for the given misorientation angle. It should be noted that the tilt axis alone is not sufficient to describe properly symmetric tilt grain boundary properties, therefore also the grain boundary

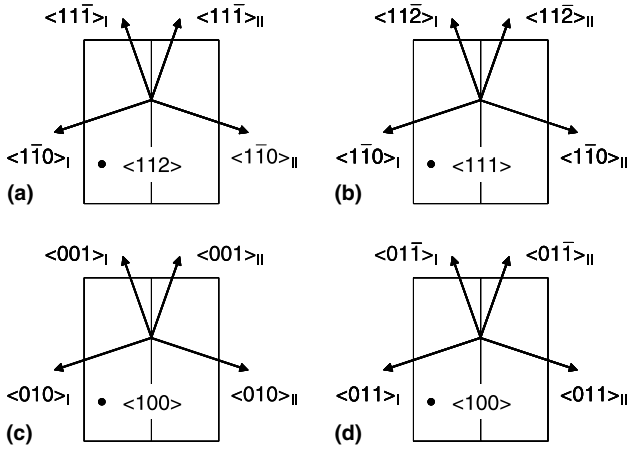

Fig. 2. Orientations of the investigated bicrystals. The rotation axis is marked by a dot. (a) ⟨1 1 2⟩-tilt grain boundaries; (b) ⟨1 1 1⟩-tilt grain boundaries; (c) ⟨1 0 0⟩ (0 1 0)-tilt grain boundaries; and (d) ⟨1 0 0⟩ (0 1 1)-tilt grain boundaries.

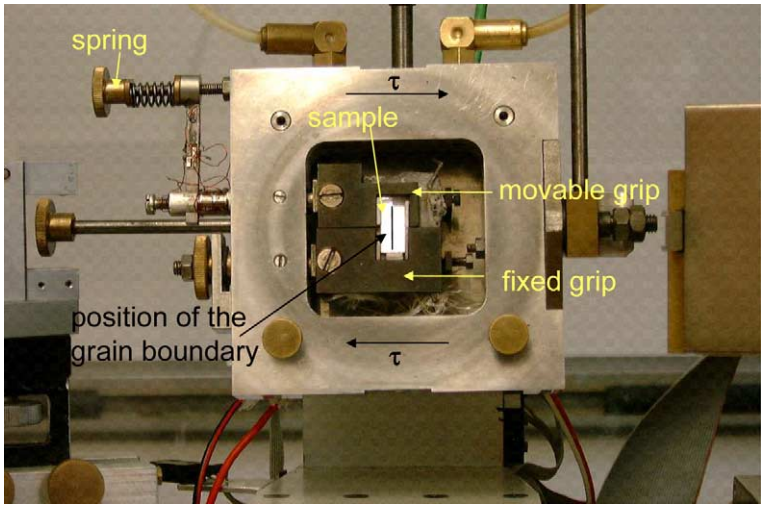

Fig. 1. Sample holder for in situ experiments on planar grain boundaries under an external stress [7].

Table 1
Average deviations from the given tilt axis and the symmetric position for the investigated tilt grain boundaries

Tilt axis/transverse direction	Average deviation from given tilt axis (°)	Average deviation from symmetric position (°)
⟨1 1 2⟩/(1 1 0)	1.62 ± 0.12	0.75 ± 0.07
⟨1 1 1⟩/(1 1 0)	1.53 ± 0.15	0.74 ± 0.05
⟨1 0 0⟩/(0 1 0)	2.63 ± 0.31	0.69 ± 0.06
⟨1 0 0⟩/(0 1 1)	2.68 ± 0.25	0.55 ± 0.05

normal, i.e. the migration direction, which is perpendicular to the tilt axis, must also be specified. Consequently, we distinguish between tilt grain boundaries with ⟨1 0 0⟩-tilt axis with a (0 1 0) grain boundary normal (Fig. 2(c)) and ⟨1 0 0⟩-tilt grain boundaries with a (0 1 1) grain boundary normal (Fig. 2(d)). We will see later that it is important to characterize properly the orientations of the two grains of the bicyrstals as well as the misorientations. For this, the bicrytsals are examined by Laue reflection method and EBSD measurements. Table 1 compiles the average deviations from the given tilt axis as well as from the symmetric position for the tilt axes investigated here.

3. Experimental results

3.1. Motion of symmetric tilt boundaries

In this section, we present the results of in situ experiments on symmetric ⟨1 0 0⟩ (0 1 1)-tilt grain boundaries under the influence of an imposed mechanical shear stress. The stress induced migration of grain boundaries with the other tilt axes is described in detail in [5–7].

Fig. 3 shows the Arrhenius plot for a planar, symmetric ⟨1 0 0⟩ (0 1 1)-tilt grain boundary with a misorientation angle of $\theta = 2.1°$. Obviously, the stress-driven grain boundary motion is a thermally activated process, so that we can determine the activation parameters for the grain boundary motion from the Arrhenius diagrams. The activation enthalpy for the motion of this low angle grain boundary is $\Delta H = 1.13 \pm 0.03$ eV, whereas the pre-exponential factor is $(7.95 \pm 0.86) \times 10^4$ m/s MPa.

Also in the case of planar, symmetric ⟨1 0 0⟩ (0 1 1)-high angle tilt grain boundaries, the motion can be induced by an external mechanical stress (Fig. 4). The activation enthalpy for the motion of a grain boundary with $\theta = 16.0°$ misorientation angle is $\Delta H = 0.66 \pm 0.03$ eV and the pre-exponential factor is $(4.42 \pm 0.38) \times 10^{-1}$ m/s MPa. For the ⟨1 1 2⟩- and ⟨1 1 1⟩-tilt grain boundaries, the activation parameters are given in [5] and for the ⟨1 0 0⟩-tilt grain boundaries, the corresponding results can be found in [7].

3.2. Activation enthalpies for stress induced grain boundary motion

As a summary of many experiments, Figs. 5–8 show the dependence of the activation enthalpies on misorientation angle for the different tilt axes. In all cases, there is a difference between the low- and high-angle regimes. For all low angle grain boundaries, a high activation enthalpy for the migration was found. At the transition, the activation enthalpy drops down to a lower value. Within the low angle regime, the activation enthalpy is constant, within the high angle regime a constant activation enthalpy was found for the investigated ⟨1 1 2⟩ and ⟨1 1 1⟩ grain boundaries. The transition occurs sharply at a certain transition angle. In Table 2 for all tilt axes, the average activation enthalpies for the low and high angle grain boundaries as well as the respective transition angles are listed.

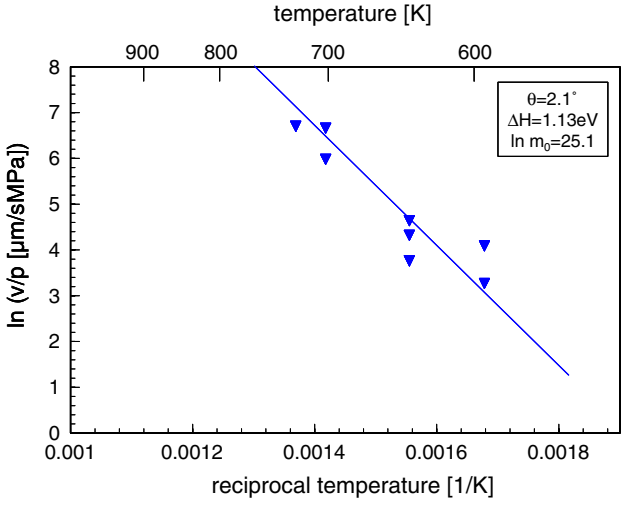

Fig. 3. Arrhenius plot for a planar, symmetrical ⟨1 0 0⟩ (0 1 1)-low angle tilt grain boundary with $\theta = 2.1°$.

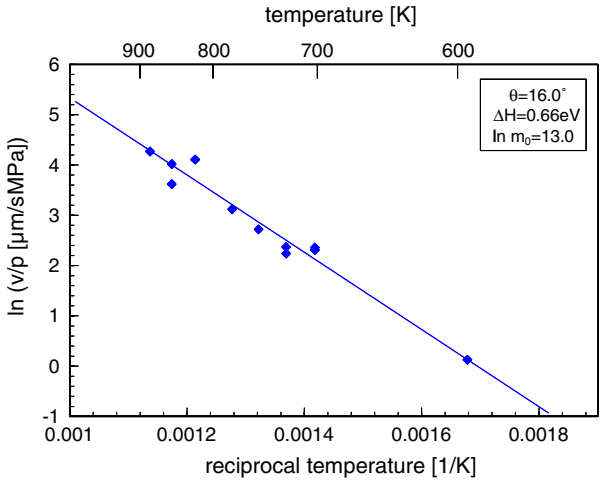

Fig. 4. Arrhenius plot for a planar symmetrical ⟨1 0 0⟩ (0 1 1)-high angle tilt grain boundary with $\theta = 16.0°$.

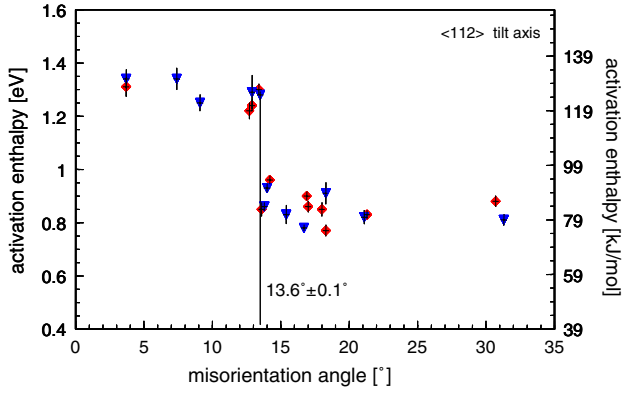

Fig. 5. Activation enthalpy vs. misorientation angle for the motion of all investigated planar, symmetric ⟨1 1 2⟩-tilt grain boundaries.

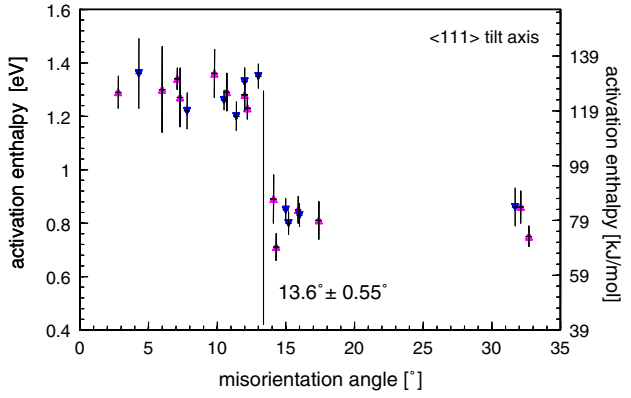

Fig. 6. Activation enthalpy vs. misorientation angle for the motion of all investigated planar, symmetric ⟨1 1 1⟩-tilt grain boundaries.

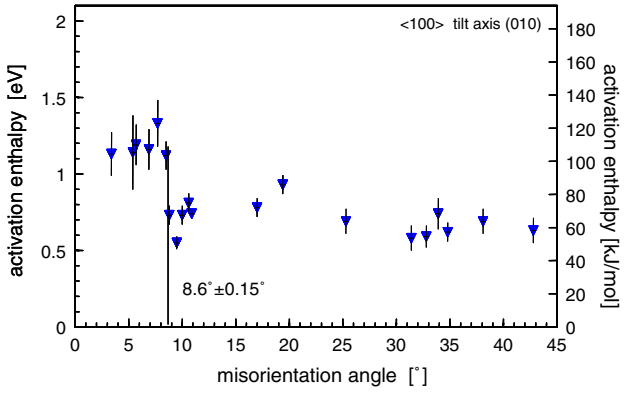

Fig. 7. Activation enthalpy vs. misorientation angle for the motion of all investigated planar, symmetric ⟨1 0 0⟩ (0 1 0)-tilt grain boundaries.

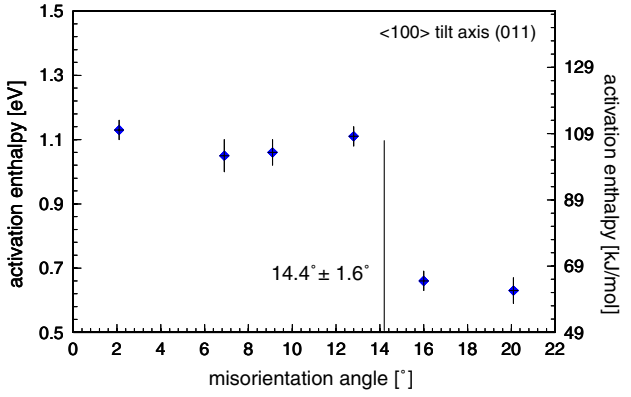

Fig. 8. Activation enthalpy vs. misorientation angle for the motion of all investigated planar, symmetric ⟨1 0 0⟩ (0 1 1)-tilt grain boundaries.

Table 2
Average activation enthalpies for grain boundary migration and transition angles for the investigated tilt grain boundaries

Tilt axis/transverse direction	Average activation enthalpy for grain boundary motion low angle grain boundaries (eV)	Average activation enthalpy for grain boundary motion high angle grain boundaries (eV)	Transition angle (°)
⟨1 1 2⟩/(1 1 0)	1.29 ± 0.01	0.86 ± 0.07	13.6 ± 0.1
⟨1 1 1⟩/(1 1 0)	1.29 ± 0.01	0.82 ± 0.02	13.6 ± 0.6
⟨1 0 0⟩/(0 1 0)	1.18 ± 0.08	0.73 ± 0.11	8.6 ± 0.15
⟨1 0 0⟩/(0 1 1)	1.09 ± 0.04	0.65 ± 0.02	14.4 ± 1.6

4. Discussion

4.1. Stress-driven grain boundary motion of tilt grain boundaries

As described in detail in [5] for ⟨1 1 2⟩- and ⟨1 1 1⟩-tilt grain boundaries and in [7] for ⟨1 0 0⟩-tilt grain boundaries, the migration mechanism of planar tilt grain boundaries under the influence of a constant shear stress can be conveniently associated with the motion of structural grain boundary dislocations. For all tilt axes, the activation enthalpy for the motion of low angle grain boundaries can be correlated with the activation enthalpy for volume diffusion in aluminium [9]. The activation enthalpies for the motion of high angle tilt grain boundaries can be associated with the respective grain boundary diffusion enthalpies [10–12]. The applied shear stress activates the glide motion of the geometrically necessary dislocations. Moreover, real boundaries are never perfect symmetric tilt boundaries but always contain structural dislocations of other Burgers vectors, as can be also seen from Table 1. These dislocations have to be displaced by non-conservative motion to make the entire boundary migrate. The climb process requires diffusion,

which can only be volume diffusion for low angle grain boundaries but grain boundary diffusion for high angle grain boundaries according to the observed activation enthalpies.

4.2. Transition from low to high angle grain boundaries

In our experiments on symmetric tilt grain boundaries, we observed a sharp change in the activation enthalpy of grain boundary mobility for all investigated tilt axes and we interpret this step as the structural transition from low angle to high angle grain boundaries.

As can be seen from Table 2, the transition angles for ⟨1 1 2⟩ and ⟨1 1 1⟩ tilt grain boundaries are the same, but the transition angle for ⟨1 0 0⟩ (0 1 0)-tilt grain boundaries is quite different, whereas the transition angle for ⟨1 0 0⟩ (0 1 1)-tilt grain boundaries is comparable to the transition angle of ⟨1 1 2⟩- and ⟨1 1 1⟩-tilt grain boundaries. How can we interpret these results?

At the transition angle, we can assume that the diffusion path for the vacancies is changed from volume to grain boundary diffusion. This change in the diffusion path depends on the dislocation distance in the grain boundary. For low angle grain boundaries, the dislocation distance is large, the dislocations can be localized as isolated dislocations. To transport vacancies which are needed for the climb process to the dislocations volume diffusion is required. For high angle grain boundaries, the distance between the dislocations is small, the dislocation cores overlap and the transport of the vacancies can be provided by grain boundary diffusion through the grain boundary plane. At the transition angle, the dislocation cores touch each other and, therefore, the dislocation distance at the transition angle is the dislocation core radius. We now assume that the dislocation distance in the grain boundary at the transition angle is the same for all tilt axes. The distance of the dislocations is correlated with the dislocation density in the grain boundary, therefore it is reasonable to postulate that there is a critical dislocation density at which the transition from low to high angle grain boundaries occurs. The dislocation density in a grain boundary consists of two parts. The first part is the dislocation density of the geometrical necessary dislocations, which can be calculated from the misorientation angle and the grain boundary normal. The second part is the dislocation density of other, redundant dislocations which exist in the grain boundary due to deviations from the ideal structure. This dislocation density can only be estimated from the measured deviations from the ideal tilt axis. In the following, we will calculate for every tilt axis the dislocation density at the transition angle taking account of the specified transition angle and the average deviations from the ideal structure.

4.2.1. ⟨1 1 2⟩-tilt grain boundaries

The transition angle is at $\theta_{\text{trans}} = 13.6 \pm 0.1°$ and the average deviation is $\Delta\theta_{112} = 1.62 \pm 0.12°$ (see Table 1). Therefore, we obtain for the dislocation density at the transition:

$$\begin{aligned}\frac{1}{d_{\text{trans}}} &= \frac{1}{d_{112}(13.6 \pm 0.1°)} + \frac{1}{d_{\text{dev}}(1.62 \pm 0.12°)},\\ &= \frac{2\sin\frac{\theta_{\text{trans}}}{2}}{\mathbf{b}_{110}} + \frac{2\sin\frac{\Delta\theta_{112}}{2}}{\mathbf{b}_{110}},\\ \frac{1}{d_{\text{trans}}} &= (9.3 \pm 0.2) \times 10^{8}\ \text{m}^{-1},\\ d_{\text{trans}} &= (1.08 \pm 0.02) \times 10^{-9}\ \text{m},\end{aligned} \tag{1}$$

where $\mathbf{b}_{110}$ is the Burgers vector with $\mathbf{b}_{110} = 2.86 \times 10^{-10}$ m.

4.2.2. ⟨1 1 1⟩-tilt grain boundaries

The transition angle is at $\theta_{\text{trans}} = 13.6 \pm 0.6°$ and the average deviation is $\Delta\theta_{111} = 1.53 \pm 0.15°$ (see Table 1). Therefore, we obtain for the dislocation density at the transition:

$$\begin{aligned}\frac{1}{d_{\text{trans}}} &= \frac{1}{d_{111}(13.6 \pm 0.6°)} + \frac{1}{d_{\text{dev}}(1.53 \pm 0.15°)},\\ &= \frac{2\sin\frac{\theta_{\text{trans}}}{2}}{\mathbf{b}_{110}} + \frac{2\sin\frac{\Delta\theta_{111}}{2}}{\mathbf{b}_{110}},\\ \frac{1}{d_{\text{trans}}} &= (9.2 \pm 0.5) \times 10^{8}\ \text{m}^{-1},\\ d_{\text{trans}} &= (1.09 \pm 0.06) \times 10^{-9}\ \text{m}.\end{aligned} \tag{2}$$

4.2.3. ⟨1 0 0⟩ (0 1 0)-tilt grain boundaries

The transition angle is at $\theta_{\text{trans}} = 8.6 \pm 0.15°$ and the average deviation is $\Delta\theta_{100} = 2.63 \pm 0.31°$ (see Table 1). Therefore, we obtain for the dislocation density at the transition:

$$\begin{aligned}\frac{1}{d_{\text{trans}}} &= \frac{2}{d_{100}(8.6 \pm 0.15°)} + \frac{1}{d_{\text{dev}}(2.63 \pm 0.31°)},\\ &= \frac{4\sin\frac{\theta_{\text{trans}}}{2}}{\mathbf{b}_{100}} + \frac{2\sin\frac{\Delta\theta_{100}}{2}}{\mathbf{b}_{110}},\\ \frac{1}{d_{\text{trans}}} &= (9.0 \pm 0.3) \times 10^{8}\ \text{m}^{-1},\\ d_{\text{trans}} &= (1.11 \pm 0.04) \times 10^{-9}\ \text{m},\end{aligned} \tag{3}$$

where $\mathbf{b}_{100}$ is the Burgers vector with $\mathbf{b}_{100} = 4.04 \times 10^{-10}$ m. The factor 2 in Eq. (3) is due to the fact that in ⟨1 0 0⟩-tilt grain boundaries the ⟨1 0 0⟩-edge dislocations can dissociate into pairs of ⟨1 1 0⟩- lattice edge dislocations [7].

4.2.4. ⟨1 0 0⟩ (0 1 1)-tilt grain boundaries

The transition angle is at $\theta_{\text{trans}} = 14.4 \pm 1.6°$ and the average deviation is $\Delta\theta_{100} = 2.68 \pm 0.25°$ (see Table 1). Therefore, we obtain for the dislocation density at the transition:

$$\frac{1}{d_{\text{trans}}} = \frac{1}{d_{100}(14.4 \pm 1.6^\circ)} + \frac{1}{d_{\text{dev}}(2.68 \pm 0.25^\circ)},$$
$$= \frac{2\sin\frac{\theta_{\text{trans}}}{2}}{\mathbf{b}_{110}} + \frac{2\sin\frac{\Delta\theta_{100}}{2}}{\mathbf{b}_{110}}, \quad (4)$$
$$\frac{1}{d_{\text{trans}}} = (10.4 \pm 1.0) \times 10^8 \text{ m}^{-1},$$
$$d_{\text{trans}} = (0.97 \pm 0.09) \times 10^{-9} \text{ m},$$

where $\mathbf{b}_{110}$ is the Burgers vector with $\mathbf{b}_{110} = 2.86 \times 10^{-10}$ m.

These calculations show that there is a good agreement between the dislocation densities at the transition from the low to the high angle regime for the different grain boundaries. However, the dislocations in ⟨1 0 0⟩-grain boundaries interact in a slightly different way than in the other grain boundaries. The lower transition angle for ⟨1 0 0⟩-tilt boundaries can be explained under the assumption that the dislocation density in the grain boundary at the transition angle is independent of the orientation and that the ⟨1 0 0⟩-edge dislocations dissociate into pairs of ⟨1 1 0⟩-lattice dislocations which was indeed observed in high resolution transmission electron microscope investigations [13].

The dislocation density of all dislocations in the grain boundary is the same at the transition angle for all grain boundaries, but the transition angle is dependent on the misorientation angle. Therefore, deviations from the ideal structure or dissociations of dislocations can change the transition angle. The dislocation density at the transition is approximately 9×10^8 m^{-1}, in the case of an ideal grain boundary structure without any deviations. Under the assumption that the dislocations are not dissociated, this corresponds to a transition angle equal to 15.07° which is in remarkable agreement with the commonly used value for instance for the Brandon criterion [3]. Nevertheless, in reality grain boundaries with ideal structures are unlikely to be observed, therefore the transition angle will vary appreciably from the theoretical value as was shown for ⟨1 0 0⟩-tilt grain boundaries. In general, it also predicts that high symmetry misorientation axes will exhibit higher transition angles whereas less symmetric axes will exhibit lower transition angles because of higher intrinsic dislocation densities for the same value of misorientation.

The variation in dislocation density is clearly essential to the prediction of the transition angle. Accordingly, the minimum dislocation density was calculated for a representative range of grain boundary types, as shown in Fig. 9. The density was estimated as the minimum density of lattice dislocations required to satisfy the misorientation according to the solution originally proposed by Frank [14] and repeated in various textbooks, e.g., Sutton and Balluffi [15]. Although general grain boundaries require three independent Burgers vectors, certain high symmetry cases may only require

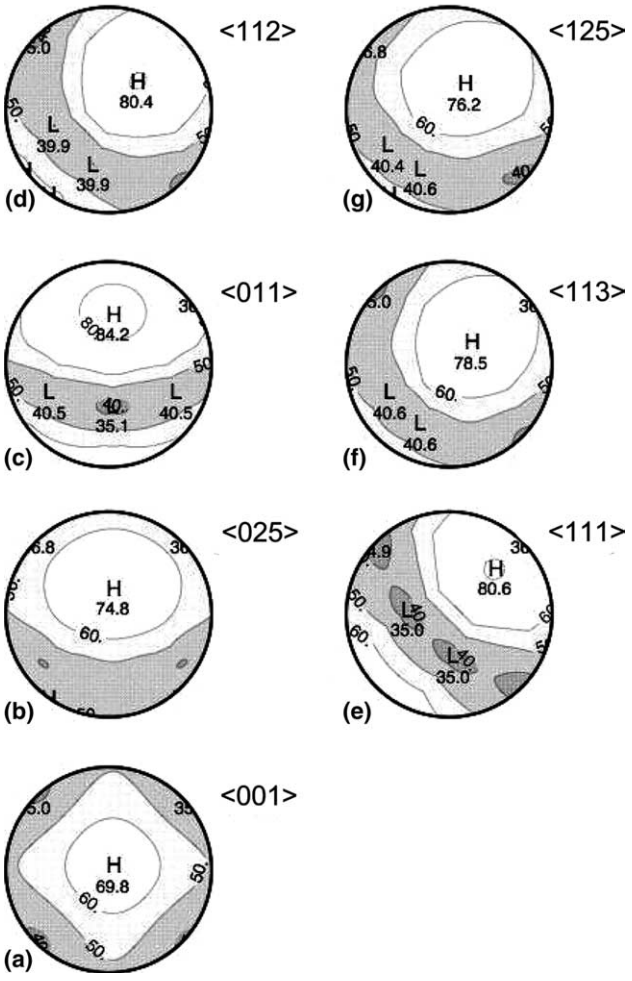

Fig. 9. Minimum dislocation density of lattice dislocations in dependence on the orientation of the grain boundary plane for different rotation axis. (a) ⟨0 0 1⟩-grain boundary; (b) ⟨0 2 5⟩-grain boundary; (c) ⟨0 1 1⟩-grain boundary; (d) ⟨1 1 2⟩-grain boundary; (e) ⟨1 1 1⟩-grain boundary; (f) ⟨1 1 3⟩-grain boundary; and (g) ⟨1 2 5⟩-grain boundary. The numbers inside the circles represent the dislocation density in arbitrary units, the larger the number is the higher the dislocation density. The highest dislocation density in each circle is marked by a "H", the lowest dislocation density is marked by a "L".

two or one Burgers vectors. Thus, three of the boundary types discussed here with (1 1 0) planes fall into the one-Burgers vector class (of symmetric tilt grain boundaries). The fourth, [0 1 1] (1 0 0) is a two-Burgers vector grain boundary. Each circle in Fig. 9 displays the variation in density for a given misorientation axis as a function of grain boundary plane. In all these cases, the misorientation axis is evident as the local maximum in density in each figure, corresponding to the pure twist grain boundary type. The minimum dislocation densities occur along the zone of pure tilt types. The minimum dislocation density invariably occurs for grain boundary planes whose normals are parallel to (or closest to) a Burgers vector, i.e. ⟨1 1 0⟩, as expected. For the two grain boundary types based on the [1 0 0] misorientation

axis, the density for the (0 0 1) plane is 42% higher than for the (0 1 1) plane.

If we compare the minimum dislocation densities for the experimentally investigated tilt grain boundaries in Fig. 9, then we can notice that for ⟨1 1 2⟩ (0 1 1), ⟨1 1 1⟩ (0 1 1) and ⟨1 0 0⟩ (0 1 1) this minimum dislocation density is nearly the same, consequently, the transition angle should be the same, because the critical dislocation density is reached for all three grain boundary types at the same misorientation angle. The minimum dislocation density for the ⟨1 0 0⟩ (0 1 0) grain boundary type is larger than for the other three grain boundary types, which means that the critical dislocation density in the ⟨1 0 0⟩ (0 1 0) grain boundary is reached at a lower misorientation angle, and therefore, the transition angle should be smaller than for the tilt grain boundaries with (0 1 1)-direction parallel (or close to) the grain boundary plane normal direction. The calculation of the dislocation density according to Frank [14] is in good agreement to the above described theoretical approach and also in good agreement with the experimental results.

5. Summary

The motion of planar low angle and high angle tilt grain boundaries can be induced by a mechanical shear stress and measured in situ. Arrhenius plots can be used to determine the activation parameters for the stress induced grain boundary motion.

The activation enthalpy for low angle grain boundaries is constant and comparable to the volume self diffusion enthalpy in aluminium. For high angle grain boundaries, the activation enthalpies for the grain boundary motion are close to the grain boundary diffusion enthalpy. Based on the different activation enthalpies for the stress induced grain boundary motion, the experiments reviewed allow a precise separation of low and high angle grain boundary behavior. Therefore, for the first time we are able to determine the transition angle very exactly by a sharp change in a physical property, namely the grain boundary mobility.

Based on the measured activation enthalpies of migration, the stress-driven motion of planar tilt grain boundaries can be associated with the climb assisted motion of the dislocations that compose the boundary.

There exists a discrete step change in the activation parameters at the transition from low angle to high angle grain boundaries. The transition is marked by a distinct step in the activation enthalpy for grain boundary motion and occurs at different angles for different tilt axes. The difference in the transition angles can be explained by the differences in dislocation structures of the grain boundaries.

Acknowledgments

One of the authors (M.W.) would like to express her gratitude to the Deutsche Forschungsgemeinschaft for financial support under contract Wi 1917/1. A.D.R. acknowledges partial support by the MRSEC program of the National Science Foundation under Award Number DMR-0079996. A.D.R. is also grateful for the hospitality of the Institut für Metallkunde und Metallphysik during his sabbatical.

References

[1] Read WT, Shockley W. Phys Rev 1950;78:275.
[2] Vold CL, Glicksman ME. In: Hu H, editor. Nature and behavior of grain boundaries. New York: Plenum Press; 1972. p. 171.
[3] Brandon DG. Acta Metall 1966;14:1479.
[4] Bauer CL. unpublished results.
[5] Winning M, Gottstein G, Shvindlerman LS. Acta Mater 2001;49:211.
[6] Winning M, Gottstein G, Shvindlerman LS. Acta Mater 2002;50:353.
[7] Winning M. Acta Mater 2003;51:6465.
[8] Czubayko U, Molodov DA, Petersen BC, Gottstein G, Shvindlerman LS. Meas Sci Technol 1995;6:947.
[9] Philibert J. Diffusion et transport de matière dans les Solides. Les Ulis Cedex: Les Éditions de Physique; 1985.
[10] Häßner A. Krist Tech 1974;9:1371.
[11] Haruyama O, Kawamoto H, Yamaguchi H, Yoshida S. Jpn J Appl Phys 1980;19:807.
[12] Volin TE, Lie KH, Baluffi RW. Acta Metall 1971;19:263.
[13] Schober T, Balluffi RW. Phys Stat Sol B 1971;44:103.
[14] Frank FC. In: Report of the symposium on the plastic deformation of crystalline solids. Pittsburgh (PA): Carnegie Institute of Technology; 1950.
[15] Sutton AP, Balluffi RW. Interfaces in crystalline materials. Oxford: Clarendon Press; 1995.